SIMULATION OF A MEMS PIEZOELECTRIC ENERGY HARVESTER INCLUDING POWER CONDITIONING AND MECHANICAL STOPPERS

Lars-Cyril Julin Blystad, Einar Halvorsen and Svein Husa
Institute for Microsystem Technology, Vestfold University College, Horten, Norway

Abstract: A piezoelectric energy harvester is simulated in SPICE, and its performance for different power conditioning techniques is presented. Mechanical stoppers are included, and their effect is investigated. The energy harvester performance is heavily dependent upon power conditioning technique. Due to the varying electrical damping, stopper influence on the energy harvester performance is strongly dependent on the type of power conditioning circuitry. We find that output power is insensitive to energy loss in the mechanical stopper for sinusoidal excitations.

Key words: Energy Harvesting, Power Conditioning, SSHI, SECE, SPICE, Piezoelectric

1. INTRODUCTION

Energy harvesting from vibration is an alternative energy source for powering low power microelectronics and microelectromechanical systems (MEMS). Three different transduction mechanisms are commonly used for the purpose of converting ambient available vibration energy into useful electrical energy: piezoelectric, electrostatic and electromagnetic [1]. In the present contribution, we investigate a piezoelectric energy harvesting system.

Maximizing the energy harvester output power and system efficiency requires optimization of the combined mechanical and electrical parts of the system. SPICE simulations results for an energy harvester with its power conversion electronics are presented in this paper. The energy harvester is represented by a lumped model with one mechanical and one electrical degree of freedom. To take into account that inertial mass deflection is limited, mechanical stoppers are included. The transducer is simulated in combination with four different power conditioning techniques, standard AC, standard DC, synchronous electric charge extraction (SECE), and synchronized switch harvesting on inductor (SSHI) [2, 3, 4].

2. ENERGY HARVESTER ARCHITECTURE

2.1 Mechanical Structure

The energy harvester is based on Aluminum Nitride (AlN) as the piezoelectric material. Although lead zirconium titanate (PZT) has a higher electromechanical coupling factor, several factors make AlN an attractive alternative. It is a simpler technology which does not require poling, is stable, and is compatible with microelectronics [5, 6]. The harvester is a beam structure with an inertial mass attached to the end. The electromechanical parameters are presented in Table 1, and correspond to the generic formulation used in [7, 8]. The equation of motion is obtained by projection onto the lowest mode of a model with several degrees of freedom.

Table 1: Electromechanical parameters

Symbol	Quantity	Value	Unit
w_b	Width of beam	4.0	mm
l_b	Length of beam	0.566	mm
m	Modal mass	17.11	mg
C_p	Clamped capacitance	122.0	pF
Q	Q-factor	350.0	
K	Stiffness	169.9	$\mathrm{N/m}$
k^2	Electromechanical coupling factor	0.6	%
ω_n	Resonance frequency	500.0	Hz
ω_a	Anti-resonance frequency	501.5	Hz

2.2 Mechanical Stoppers

Whenever inertial mass deflection reaches its limit, the mass will hit a mechanical stopper. For large amplitude vibrations it is expect that the mass will hit the stoppers frequently, and thus they have to be included in the simulation model. We choose to model the mechanical stoppers as a parallel spring dashpot system, see Fig.1a, which are in effect whenever center of mass deflection exceeds 100μm.

As the kinetic energy of the proof mass is proportional to the square of its velocity, the energy loss during stopper impact can be quantified by introducing the coefficient of restitution [9], $e = -\frac{v_1}{v_0}$ where v_1 is mass release velocity and v_0 is mass velocity at impact. Elastic and inelastic impact have coefficient of restitution $e = 1$ and

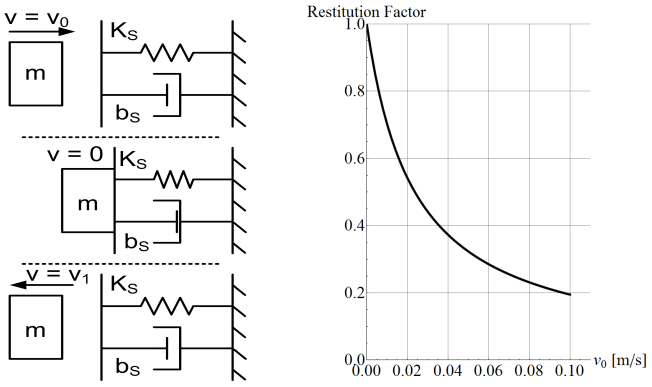

(a) *Stopper model* (b) *Coefficient of Restitution*

Fig. 1: Stopper model and coefficient of restitution

$e < 1$, respectively.

As an example, consider stoppers that give critical damping. Then stopper displacement $x_m(t)$ can be expressed as in (1) under open circuit conditions.

$$x_m(t) = \frac{a_0}{\omega_1^2}\left[-1 + \exp(-\omega_1 t)\left(1 + \omega_1 t + \frac{v_0\ \omega_1^2\ t}{a_0}\right)\right] \quad (1)$$

Here, ω_1 is the mechanical resonance frequency of the combined stopper-beam-mass system, and a_0 is the contribution to the acceleration due to the beam at stopper impact. From this, we obtain the coefficient of restitution as shown in Fig.1b. Clearly it is dependent on impact velocity, and therefore not so suitable as a control parameter for the simulations. We have therefore chosen to investigate only the cases: elastic, critically damped and completely inelastic impacts. An alternative would have been to parametrize the stoppers by e in the absence of the beam, but that would not describe the physical situation during impact.

3. SIMULATIONS

System simulations are done using four different power conditioning methods, standard AC, standard DC, SECE, and SSHI. Simulations shows that maximum output power is reached at resonance for standard AC, standard DC, and SSHI, but at anti-resonance for SECE. Simulations presented are done using optimum frequency.

3.1 Power Conditioning Circuits

Standard AC is the simplest form of power conditioning, connecting a resistive load directly between the two transducer electrodes. Standard DC rectifies the transducer output through a full bridge diode rectifier, and connects a resistive load in parallel with a storage capacitor at the output of the rectifier. SECE includes a full bridge diode rectifier followed by a Buck-Boost configuration with a modified synchronous and low frequency switching technique. The Buck-Boost switch closes on mass deflection extremes, and opens when all the charge on the transducer capacitance is emptied into the inductor [3]. It has a resistive load in parallel with a storage capacitor. SSHI consists of a series inductor and switch in parallel with the transducer capacitance. It is followed by a full bridge diode rectifier and a resistive load in parallel with a storage capacitor. The switch is closed on transducer capacitance voltage extremes, and opens after half a resonance period defined by the resonant series inductor – transducer capacitance circuit. Switching effectively inverts the voltage on the transducer capacitance, leading to a more effective transduction [4].

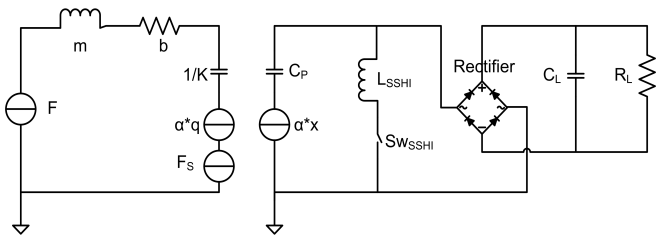

Fig. 2: Energy harvester simulation model including mechanical part and SSHI power conditioning

3.2 System Simulations

Sinusoidal excitation simulations shows little difference (<5%) using elastic, critically damped or completely inelastic stopper models. Further simulations are done using critically damped stopper model. Fig.2 shows a simulation model including both the mechanical part, the electromechanical coupling and a SSHI power conditioning circuit, where F is the external force acting on the system, b is the damping constant, q is the charge on the transducer electrode, $\alpha = \sqrt{\frac{K}{C_P}}k$ is the force factor, F_S is the mechanical stopper force, x is the displacement, L_{SSHI} is the SSHI inductor, SW_{SSHI} is the SSHI switch, C_L is the storage capacitance, and R_L is the load resistance. The remaining symbols corresponds to parameters defined in Table 1. Fig.3 shows output power vs. load resistance at low acceleration, 0.25g. Maximum mass deflection is not reached, and stoppers are not in effect. As expected, the output power using SECE is independent of the load resistance over a large range, while the other configurations have an optimum low acceleration load. Fig.4 shows output power vs. load resistance at high acceleration, 4.0g. Maximum deflection is now reached, and stoppers are frequently in effect.

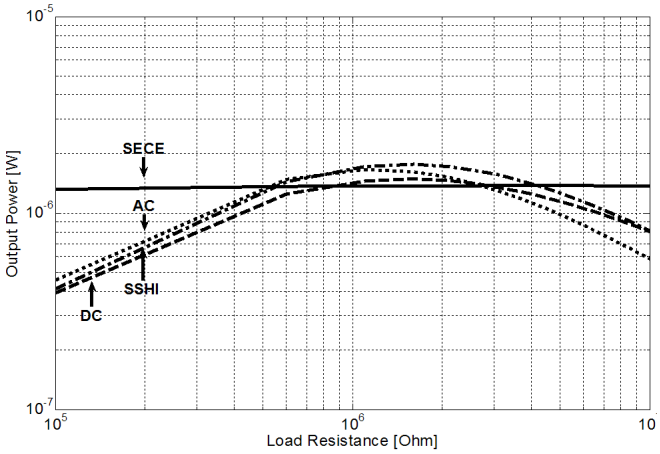

Fig. 3: Output power vs. load resistance at constant acceleration 0.25g

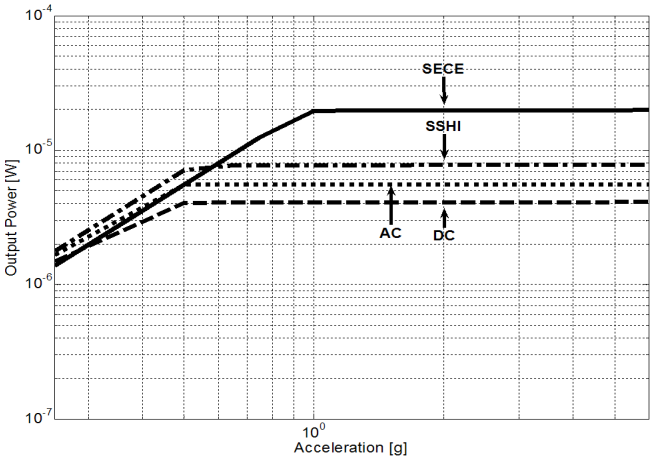

Fig. 5: Output power vs. acceleration with constant resistance optimized for low acceleration

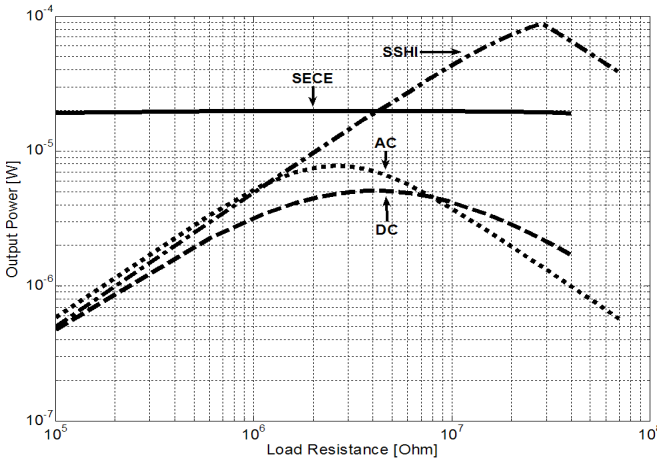

Fig. 4: Output power vs. load resistance at constant acceleration 4.0g

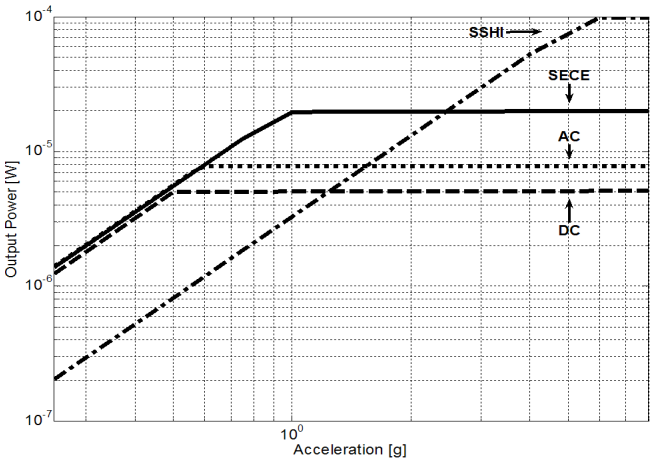

Fig. 6: Output power vs. acceleration with constant resistance optimized for high acceleration

SECE output power is still independent of load resistance over a large range, while for AC and DC configurations the optimum load resistance is increased. SSHI output power increases with increasing load resistance, but only as long as the stoppers are in effect. Fig.5 and 6 shows that with constant output load the output power for all four power conditioning methods reaches a maximum level at some acceleration and does not increase further with increase in acceleration. Maximum power level is not the same using different techniques. SECE is the only technique that shows independence of load resistance over a large range. With constant load resistance optimized for high accelerations, in the flat region SSHI gives five times higher maximum output power than SECE, and approximately 12 and 19 times higher than AC and DC respectively. In this case SSHI has a relatively high output voltage, which is in the range of 70V, while SECE has approximately 8.5V, DC has approximately 4.5V, and AC has approximately $\pm$ 6.5V output voltage. The high SSHI output voltage can be a limiting factor for its practical usage. Compared to SECE, the optimal high acceleration load resistance for SSHI is at least one order of magnitude higher, which gives approximately 3 times the output voltage for the same output power. Fig.7 shows how the stopper force acts on the inertial mass as a function of load resistance for various accelerations using AC and SSHI. Combined with Fig.8 it shows that for SSHI, increasing the load resistance gives an increase in the output power, as long as the stoppers are in effect.

4. DISCUSSION

Sophisticated power conditioning circuits, e.g. SECE and SSHI, uses active circuits and are in need of some control circuits. Power consumption used for power con-

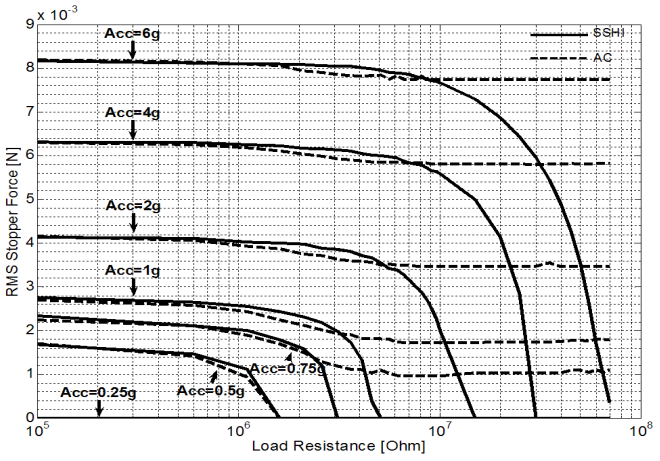

Fig. 7: Critically damped mechanical stopper force vs. load resistance for standard AC and SSHI

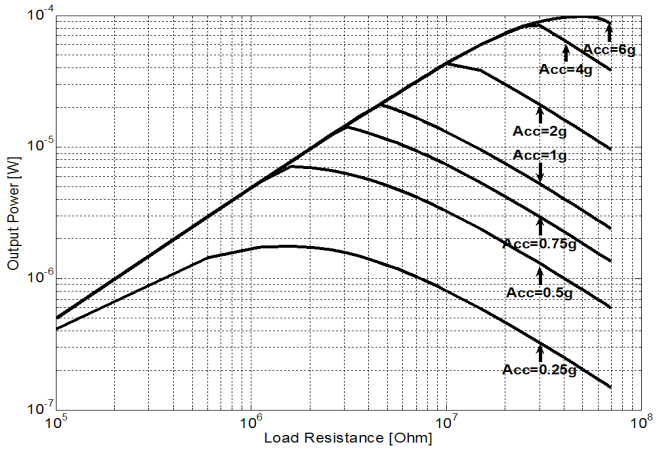

Fig. 8: Output power vs. load resistance at varying acceleration for SSHI

ditioning is not considered in this paper, although it may be significant. Literature reports power conditioning power consumption in the order of μW. Thus power conditioning technique must be chosen dependent on the specific application environment, and expected total harvested energy.

Using the same transducer with different power conditioning techniques, maximum mass deflection is the same. SSHI gives the largest electromechanical damping, and thus can be driven at higher accelerations before the stoppers comes into effect, compared to the other techniques. This leads to the largest harvested energy, but SSHI is load dependent, and needs load control for optimization. SECE on the other hand is load independent over a large range, and gives most power over a large range of loads. AC and DC techniques is preferred only when very low accelerations are expected, thus stoppers will not be in effect and power overhead will not be sufficient to drive an active power conditioning circuit.

5. CONCLUSION

SECE is promising at low accelerations and at high accelerations under variable load resistance. With reservations concerning the high output voltage of SSHI, the technique seems preferable at high accelerations with load control. AC and DC techniques should be used at low acceleration which results in insufficient overhead output power to drive active circuits.

REFERENCES

[1] Beeby S P, Tudor M J, White N M 2006 Energy harvesting vibration sources for microsystems applications *Meas. Sci. Technol.*, **17** R175–R195

[2] Guyomar D, Richard C, Lefeuvre E, Petit L 2004 Piezoelectric non-linear systems for standalone vibration control and energy reclamation *Adaptronic Congress (Hildesheim, Germany, 27–28 April 2004)*

[3] Lefeuvre E, Badel A, Richard C, Guyomar D 2005 Piezoelectric energy harvesting device optimization by synchronous electric charge extraction *J. Intell. Mater. Syst. Struct.* **16** 865–876

[4] Badel A, Guyomar D, Lefeuvre E, Richard C 2006 Piezoelectric energy harvesting using a synchronized switch technique *J. Intell. Mater. Syst. Struct.* **17** 831–839

[5] Marzencki M, Ammar Y, Basrour S 2007 Integrated power harvesting system including a mems generator and a power management circuit *TRANSDUCERS'07 (Lyon, France, 10-14 June 2007)* 887–890

[6] Marzencki M, Ammar A, Basrour S 2007 Design, fabrication and characterization of a piezoelectric microgenerator including a power management circuit *DTIP 2007, Symposium on Design, Test, Integration and Packaging of MEMS/MOEMS (Stresa, Italy, 25-27 April 2007)* 350–353

[7] Halvorsen E 2007 Broadband excitation of resonant energy harvesters *Technical Digest PowerMEMS 2007 (Freiburg, Germany, 28-29 November 2007)* 319–322

[8] Halvorsen E 2008 Energy harvester driven by broadband random vibrations *J. Microelectromech. S.* DOI:10.1109/JMEMS.2008.928709

[9] Timoshenko S, Young D H 1956 *Engineering Mechanics* (Singapore, McGraw-Hill Book Co.)